Available online at www.sciencedirect.com

ScienceDirect

Advances in Space Research 69 (2022) 823–836

ADVANCES IN SPACE RESEARCH (a COSPAR publication)

www.elsevier.com/locate/asr

Scientific objectives and payloads of the lunar sample return mission—Chang'E-5

Changyi Zhou [a], Yingzhuo Jia [a,*], Jianzhong Liu [b], Huijun Li [a], Yu Fan [a], Zhanlan Zhang [a], Yang Liu [a,c], Yuanyuan Jiang [a], Bin Zhou [d], Zhiping He [e], Jianfeng Yang [f], Yongfu Hu [g], Zhenghao Liu [a,h], Lang Qin [a,h], Bohan Lv [a], Zhongliang Fu [i], Jun Yan [j], Chi Wang [a,c], Yongliao Zou [a,c,*]

[a] National Space Science Center, Chinese Academy of Sciences, Beijing 100190, China
[b] Institute of Geochemistry, Chinese Academy of Sciences, Guiyang 550002, China
[c] State Key Laboratory of Space Weather, National Space Science Center, Chinese Academy of Sciences, Beijing 100190, China
[d] Aerospace Information Research Institute, Chinese Academy of Sciences, Beijing 100094, China
[e] Shanghai Institute of Technical Physics, Chinese Academy of Sciences, Shanghai 200083, China
[f] Xian Institute of Optic and Precision Mechanic, Chinese Academy of Sciences, Xian 710119, China
[g] Beijing Institute of Space Mechanics and Electricity, China Academy of Space Technology, Beijing 100076, China
[h] University of Chinese Academy of Science, Beijing 100049, China
[i] Lunar Exploration and Space Engineering Center, China National Space Administration, Beijing 100190, China
[j] National Astronomical Observatories, Chinese Academy of Sciences, Beijing 100012, China

Received 6 December 2020; received in revised form 10 August 2021; accepted 5 September 2021
Available online 16 September 2021

Abstract

In the early morning on December 17, 2020 Beijing time, China's chang'E-5 probe successfully returned to the Earth with 1731 g of lunar samples after completing drilling, shoveling, packaging of lunar soil and scientific exploration on lunar surface. It is the successful completion of the third phase of China's lunar exploration project, namely "circling, landing and returning to the moon". The scientific objectives of CE-5 mission are to carry out in situ investigation and analysis of the lunar landing region, laboratory research and analysis of lunar return samples.

This paper analyzes scientific exploration tasks of CE-5 mission conducted on the lunar surface, and carries out the scientific payload system architecture design and individual scientific payload design with the scientific exploration task requirements as the target, and proposes the working mode and main technical index requirements of the scientific payloads. Based on the preliminary geological background study of the Mons Ruemker region which is the landing region of CE-5, the lunar scientific exploration and the laboratory physicochemical characterization of the return samples are of great scientific significance for our in-depth understanding of the formation and evolution of the Earth-Moon system and the chemical evolution history of the lunar surface.

Keywords: CE-5; Scientific objectives; Scientific payloads; Lunar sample

1. Introduction

The Moon, being our only natural satellite, is the closest celestial body to the Earth. Since the 1960s, more than 100 probes have been sent to the moon. When American astro-

* Corresponding authors.
E-mail addresses: jiayingzhuo@nssc.ac.cn (Y. Jia), zouyongliao@nssc.ac.cn (Y. Zou).

https://doi.org/10.1016/j.asr.2021.09.001
0273-1177/

naut Armstrong stepped on the moon on July 20, 1969, the human dream of exploring the vast space was greatly inspired. From then on, there were 6 probes and 12 astronauts landed on the moon, and 382 kg of lunar rock and soil samples were carried back to earth. As well, the inspection and sampling return of the Soviet Union unmanned probe, set off the lunar probing upsurge. Through these explorations, we have had a more systematic and comprehensive understanding of the lunar morphology, rock composition, etc., recorded the moon quakes, and prospected the interior of the moon.

China Lunar Exploration Program (CLEP) named "Chang'E Program" in 2004, was divided strategically into three phases: Orbiting, Landing and Robotic Sample Return. Phase I of CLEP: from 2004 to 2008, was to achieve a global orbiting detection of the moon; Phase II of CLEP: from 2008 to 2014, was to achieve soft landing on the moon surface, in situ exploration and patrol detection; Phase III of CLEP: from 2011 to 2020, was to achieve robotic sample return from the moon (Pei et al., 2015; Luan, 2006). Starting from Chang'E-1 mission, China has implemented five successful lunar missions, including Chang'E-1, 2,3,4,5 (Ye et al., 2014). Fig. 1 shows China's lunar exploration program three phases, and Table 1 shows the scientific objectives and payloads of China's Chang'E series missions.

Chang'E-1 (CE-1) and Chang'E-2 (CE-2) probes were launched in 2007 and 2010, respectively. These two missions achieved a global and general remote sensing exploration of the moon, obtained the world's first all coverage "microwave map of the moon", made the lunar holographic image with a resolution better than 7 m, and detected the distribution and abundance of elements on the lunar surface (Ouyang et al., 2008; Liu et al., 2013). CE-2 probe made preparation for the soft-landing on the moon, which was the objective of second phase.CE-2 probe surveyed the preselected landing site of CE-3 in detail, and even further probed the second Lagrangian (L2) point and Asteroid 4179 Tutatis (Jianjun et al., 2013).

Chang'E-3(CE-3) probe was launched on December 2, 2012, and soft landed successfully at northwest Mare Imbrium of the moon on December 14, then the Yutu rover separated from the lander. This site was named "Guanghangong". CE-3 probe investigated the topography and geological structure of lunar surface (Le et al., 2014), mineralogical composition (Zhao et al., 2014) and lunar internal structure (Fa et al., 2014, 2015), detected the earth's plasma layer (He et al., 2013), and carried out lunar-based optical astronomical observation (Wang et al., 2011). CE-3 probe is still working on the scientific detection, which is the longest working probe on the moon.

Chang'E-4(CE-4) probe was launched on December 8, 2018, and landed in Von Karman Crater inside the South Pole-Aitken basin on the far side of the moon on January 3, 2019. CE-4 mission is the first mission to make a soft landing and perform scientific exploration on the far side of the moon (Jia et al., 2018). It discovered the deep lunar material (LING et al., 2019), and revealed the geological evolution history of the area. For the first time in the world, the radiation characteristics and energy spectrum structure of high energy particles and neutral atoms on the lunar surface were obtained (Zhang et al., 2020a). By March 2021, CE-4 probe had been working for 28 months, the total mileage of Yutu-2 rover is 652.62 m.

Chang'E-5(CE-5) probe was launched on November 24, 2020, by a Long March-5 rocket (CZ-5) at Wenchang Space Launch Center in Hainan province. CE-5 probe took back 1731 g of lunar samples, and the samples have been transferred to research teams for further study. With the

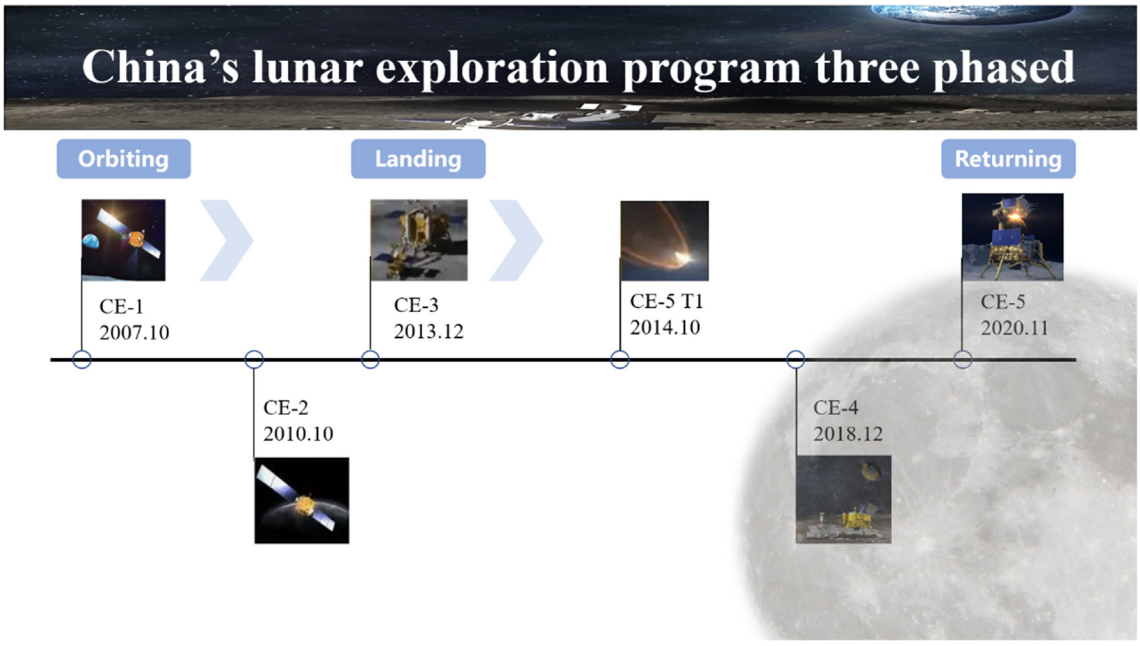

Fig. 1. China's lunar exploration program three phased.

Table 1
Scientific objectives and payloads of China's Chang 'E series missions.

Mission	Scientific Objectives	Scientific Payloads
CE-1	1) 3D image acquisition of the lunar surface; 2) The distribution characteristics of elements and mineral types study on the lunar surface; 3) Lunar soil properties detection; 4) Earth-lunar space environment exploration.	CCD Stereo Camera Laser Altimeter Interferometric Imaging Spectrometer γ-ray Spectrometer X-ray Spectrometer Microwave Detector High Energy Particle Detector Solar Wind Ion Sounder
CE-2	1) 3D image acquisition of the lunar surface, resolution is better than 10 m; 2) Lunar mineral composition exploration; 3) Lunar soil properties detection; 4) Earth-lunar space environment exploration.	CCD Stereo Camera Laser Altimeter γ-ray Spectrometer X-ray Spectrometer Microwave Detector High Energy Particle Detector Solar Wind Ion Sounder
CE-3	1) Lunar surface topographic and geological structure investigation; 2) Lunar surface mineralogical composition and available resource exploration; 3) Earth plasma extreme ultraviolet observation and lunar based optical astronomical observation.	Terrain Camera Landing Camera Extreme Ultraviolet Imager Lunar Optical Telescope Panoramic Camera Lunar Penetrating Radar X-Ray Spectrometer Acousto-Optic Spectrometer
CE-4	1) Low-frequency radio astronomical study on the lunar surface; 2) Shallow structure investigation on the roving area of the far side of the moon; 3) The topographic and the mineralogical composition investigation on the roving area of the far side of the moon; 4) Neutrons radiation dose and neutral atoms study on lunar environment.	Terrain Camera Landing Camera Low Frequency Spectrometer Panoramic Camera Visible and Near-Infrared Imaging Spectrometer Lunar Lander Neutrons and Dosimetry Advanced Small Analyzer for Neutrals Netherlands-China Low-Frequency Explorer

successful completion of the CE-5 mission, the target on three phases of China's lunar exploration project is totally achieved (Ye et al., 2014).

2. CE-5 mission

2.1. Process of CE-5 mission

CE-5 probe consists of an ascender, a lander, a returner and an orbiter, with a total weight of 8.2 tons. It is the first Chinese spacecraft to implement an unmanned lunar surface sample return mission. It is why CE-5 was launched by the Long March-5 rocket-currently China's most capable carrier, and sent into Earth-Moon transfer orbit from Wenchang Space Launch Center in Hainan province which has the higher tangential speed.

The flight process of CE-5 had 11 stages. After the separation of the probe and the launch vehicle, the probe had about 5 days of earth-moon transfer flight, arrived at perilune and performed 2 near-moon brakes, then entered the circular lunar orbit with an altitude of 200 km. In the circumlunar orbit, the probe separated from the orbiter-returner combination and the lander-ascender combination, where the orbiter-returner combination continued to fly in a 200 km circular orbit. In the meantime, the lander-ascender combination completed two descents and decelerated into a 15 km*200 km elliptical orbit at the right time, then implemented a powered descent and a soft landing on the lunar surface at the right time.

The lander-ascender combination started soft landing on the lunar surface from the initial point of descent, and found a suitable time to decelerate and hover for obstacle avoidance during the descent. The whole process of landing and descent lasted about 15 min. After touchdown, the lander-ascender combination stayed on the lunar surface for about 48 h. It completed the drilling and shoveling lunar soils and encapsulation work, meanwhile, the scientific payloads conducted scientific exploration on the lunar surface. At the same time, the orbiter-returner combination still running in circumlunar orbit and performed several orbital maneuvers to prepare for the subsequent lunar orbit rendezvous and the samples transfer.

After the lunar sample collection and encapsulation, the lander and ascender were unlocked and separated, and the ascender engine ignited and took off, entering the target orbit of 15 km*180 km. Through remote guidance and proximity guidance, the ascender and the orbiter-returner combination completed unmanned rendezvous and docking, and the sealed encapsulation device was transferred from the ascender to the sample module in returner, after which the orbiter-returner combination was safely separated from the ascender.

After separation, the orbiter-returner combination made orbital adjustment and implemented acceleration maneuvers to enter the lunar-earth transfer orbit, and orbiter-returner combination separated at an altitude about 5000 km from the ground, the orbiter performed evasive maneuvers, and the returner went through inertial glide and then found a suitable node to achieve re-entry into the Earth's atmosphere. In this process, the returner first re-entered the Earth's atmosphere in a speed close to the second cosmic velocity, completed atmospheric deceleration by way of a semi-ballistic jump return, opened its parachute at a distance of about 10 km from the ground and landed at the scheduled location (Chen et al., 2015). Fig. 2 shows the composition of CE-5 probe (Ye et al., 2014), Fig. 3 shows the process of CE-5 mission (Zhihao, 2021).

2.2. Scientific objectives

The goals of CE-5 mission are to land on the lunar surface, collect a total 2 kg of lunar regolith samples from depths up to ~2 m through gathering and drilling, return the samples back to the earth, and study the samples in ground laboratory. Two scientific objectives of CE-5 mission are as below:

(1) To carry out in situ exploration in sample collection area, provide the evidence to selectively collect samples and establish the connection between the data acquired on the moon and analyzed in ground laboratory.
(2) To systematic and long-term study about the lunar regolith samples in ground lab, analyze the structure, physical properties and substance composition of lunar samples and research the origin and evolution history of the moon.

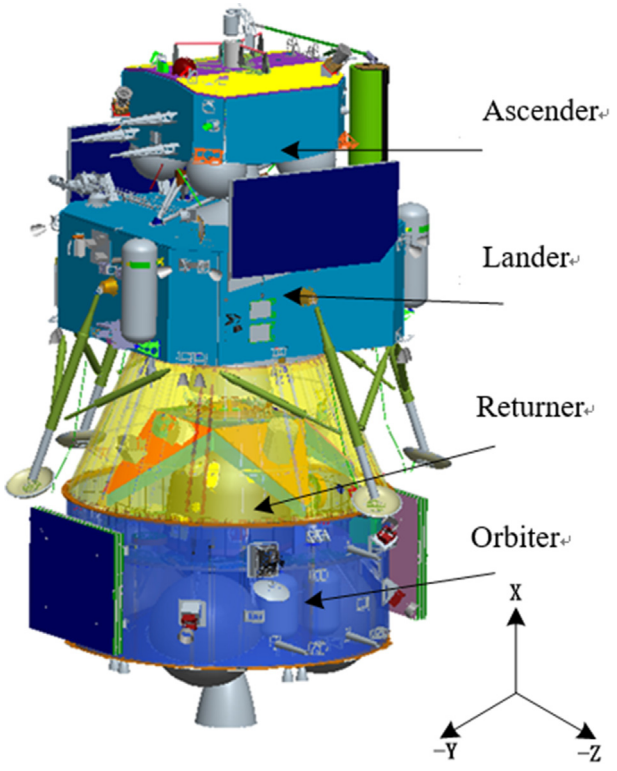

Fig. 2. The composition of CE-5 probe. The orbiter -returner combination was at the bottom, the lander-ascender combination was on the top (Ye et al., 2014).

To achieve the first scientific objectives, there were 4 scientific payloads installed on the lander, which were Landing Camera (LCAM), Panoramic Cameras (PCAM), Lunar Mineralogical Spectrometer (LMS) and Lunar Regolith Penetrating Radar (LRPR). Together with the payload controller on the lander, they constituted the scientific payload system.

The LCAM and PCAM jointly completed the research on lunar surface topography and geological structure. The LCAM took video during the powered descending phase to acquire images of the lunar topographic feature of the landing area. The PCAM were used to acquire high solution lunar images of landing region and sample collection area, and provide images to help the decision-making process of gathering samples collection.

The LMS was used to survey the composition and resources of the lunar surface. The LMS would acquire the visible and infrared spectral images data before gathering samples collection (original lunar soils). After gathering samples collection (fresh lunar soil), the LMS would conduct in situ analysis of mineral composition and distribution on samples collection area, and provide information to help the decision-making process of gathering samples collection.

The LRPR was used to detect the lunar subsurface structure. The LRPR would acquire the information of lunar soil layering and structure of drilling area before drilling samples collection, analyze the structural features of samples and help the decision-making process of drilling samples collection. Table 2 shows the relationship between scientific exploration tasks and scientific payloads.

2.3. Landing region

The CE-5 probe landed in the Mons Ruemker region (43.1° N,51.6° W) of northern Oceanus Procellarum, which was an area none probes ever landed before (Mallapaty, 2020).Fig. 4 shows the landing sites of CE-5 mission, Apollo mission and Luna mission of the Soviet Union. The area is covered by widespread mare basalts, and contains a variety of geomorphology including impact craters, wrinkle ridges, sinuous rilles, and volcanic domes. Analysis of young mare basalt samples from this region will significantly improve the lunar chronology by calibrating the lunar cratering rate in the last three billion years and provide exact absolute radiometric dates for some of the Moon's most young volcanic events. The lunar samples retrieved by the U.S and the Soviet Union lunar missions,

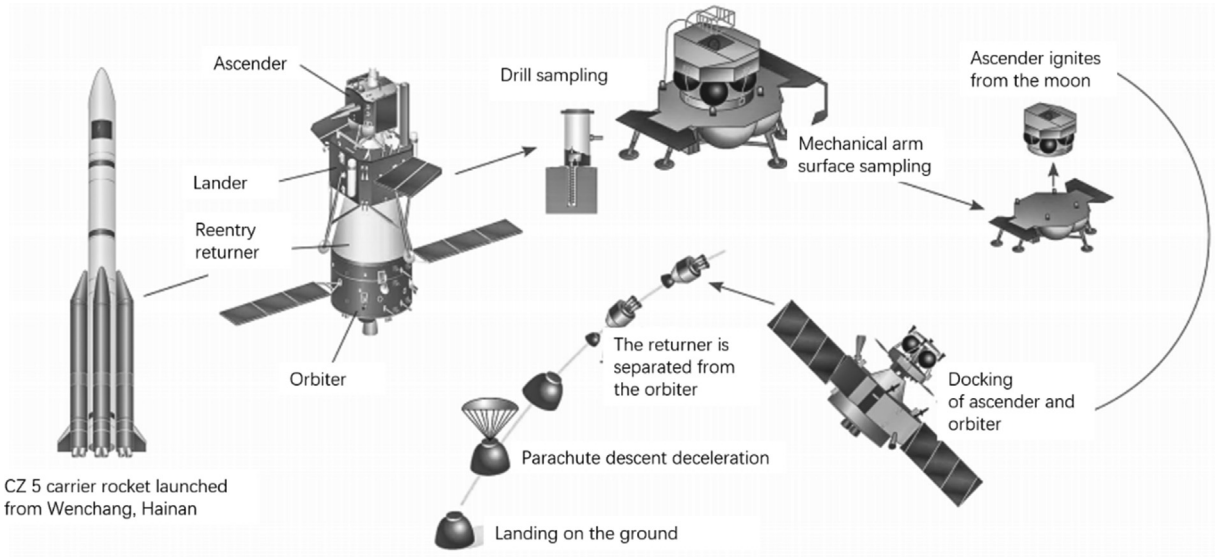

Fig. 3. The process of CE-5 mission (Zhihao, 2021).

Table 2
The relationship between scientific exploration tasks and scientific payloads.

Exploration Tasks	Scientific Payloads
1) To investigate the lunar surface topography and geological structure	PCAM
2) To provide the images to help the progress of samples collection	
3) To select the points to gather lunar samples	
To investigate the lunar surface topography and geological structure during the descent landing process	LCAM
To survey the substance composition and resource of lunar surface	LMS
1) To detect the lunar subsurface structure	LRPR
2) To support the process of drilling samples collection	

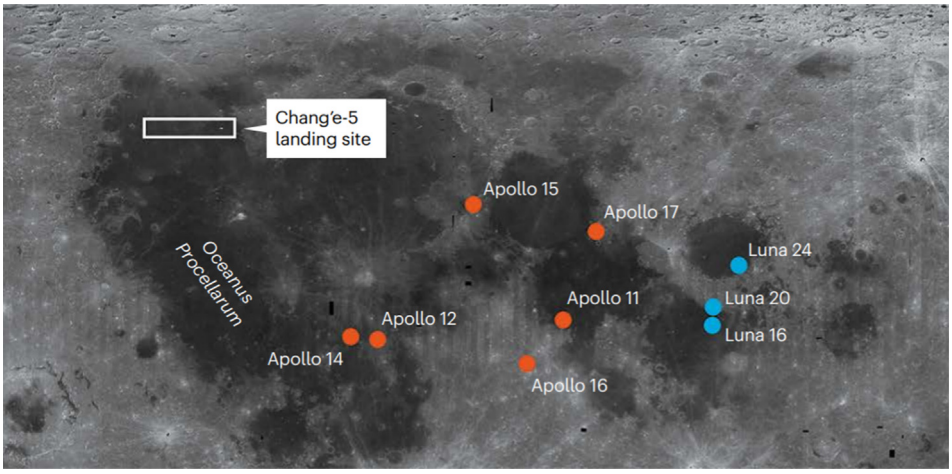

Fig. 4. The landing region of CE-5, Apollo and Luna.

are all older than 3 billion years. Scientists believe that lunar volcanic activity peaked 3.5 billion years ago, then gradually weakened and stopped, while volcanic activity on the earth is still very active. Based on the analysis of remote sensing data, it is believed that some areas of the moon, including the CE-5 landing area, may contain volcanic lava formed only last 1–2 billion years ago. At present, there are no samples of the moon in this period, which will be achieved by CE-5 mission (Qian et al., 2018; Qian et al., 2020). If the lunar sample of CE-5 proves that the moon is still active during this period, it will have important scientific value for the lunar volcanism, especially for the lunar evolution (Mallapaty, 2020). In addition, this region also includes the Procellarum KREEP

Terrane (PKT), which has high concentrations of radiogenic heat-producing elements (e.g. Th, U, and K) (e.g. Lucey et al., 2006). These samples will also help us understand how the radioactive PKT materials have contributed to the formation of late-stage mare volcanism.

In addition, this region also includes the Procellarum KREEP Terrane (PKT), which has high concentrations of radiogenic heat-producing elements (e.g. Th, U, and K) (e.g. Lucey et al., 2006). These samples will also help us understand how the radioactive PKT materials have contributed to the formation of late-stage mare volcanism. The Mons Ruemker Region is shown in Fig. 5.

3. Scientific payloads

3.1. Framework of scientific payloads system

With the scientific payload controller as the core, scientific payload subsystem formed each scientific payload a system through the internal bus network. The payload controller unified interface with the satellite platform, to provide each scientific payload unified power supply, command control, data acquisition, processing and caching. Under the control of the payload controller, each scientific payload carried out scientific exploration, and the scientific payload subsystem achieved the autonomous operation in orbit, and had the ability of independent health management and fault repair capabilities.

The electric design of the payload controller, Panoramic Cameras and Lunar Mineralogical Spectrometer were integrated in the scientific payload system. 1553B bus communication was used between the payload controller and data management system of the lander platform. Payload controller supplied electricity for Panoramic Cameras and Lunar Mineralogical Spectrometer, processed the data received from them and transferred the data to the lander platform by LVDS channel.

Lunar Regolith Penetrating Radar was away from other payloads, the working timing sequence of Landing Camera was different from others. This two payloads were directly connected to the lander platform and respectively had the primary bus power and command power to receive and execute switching commands from the lander. Through 1553B bus interface connected to dada management subsystem of the lander, Lunar Regolith Penetrating Radar could receive data injection commands and send detection data and engineering parameters. After powered on, Landing Camera could send detection data through LVDS interface with the dada management subsystem of the lander. Fig. 6 shows the Framework of scientific payload system, Fig. 7 shows the pictures of the scientific payloads.

3.2. Work mode of scientific payloads

In order to effectively achieve the scientific exploration objectives, the detection requirements of scientific payloads are: 1) to obtain the panoramic camera full field of view detection data before lunar sample shoveling collection in order to analyze the sampling area; 2) to obtain the Lunar Mineralogical Spectrometer full field of view detection data (original surface of lunar soil) before lunar sample shoveling collection; 3) to obtain the lunar sample shoveling collection full field of view detection data (fresh surface of lunar soil) after lunar sample shoveling collection; 4) to obtain Lunar Regolith Penetrating Radar data before drilling to analyze the characters of the geological structure of the drilling area.

Based on the above requirements, the scientific payloads working modes are designed as follows:

The scientific payloads don‘t work in the probe launch segment, the Earth-Moon transfer segment, the circumlunar segment, and the landing impact segment.

The Landing camera: works during the lander powered descent section to obtain optical images of the landing area, and the working time is no longer than 30 min. There are two working modes, mode 1 effective image element number 2352 × 1728, image compression ratio 4:1, mode 2 effective image element number 1024 × 1024, image compression ratio 8:1, both generate 1 image per second. After

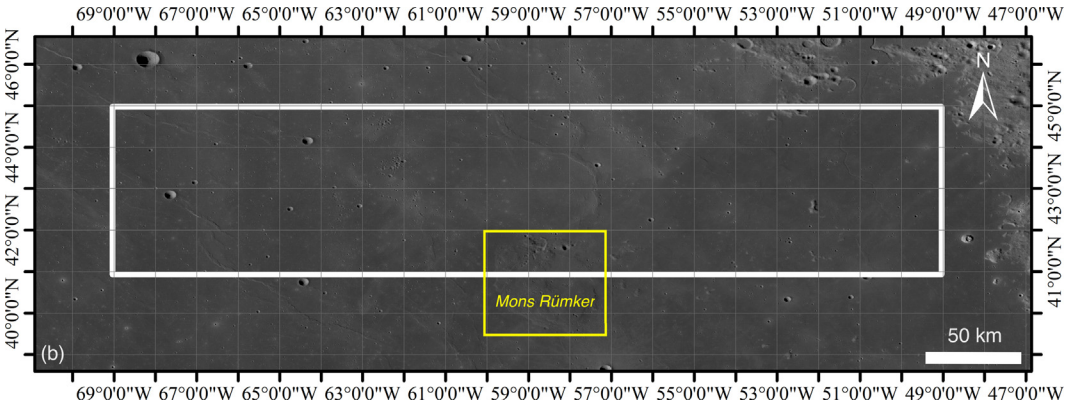

Fig. 5. The landing region—the Mons Ruemker Region.

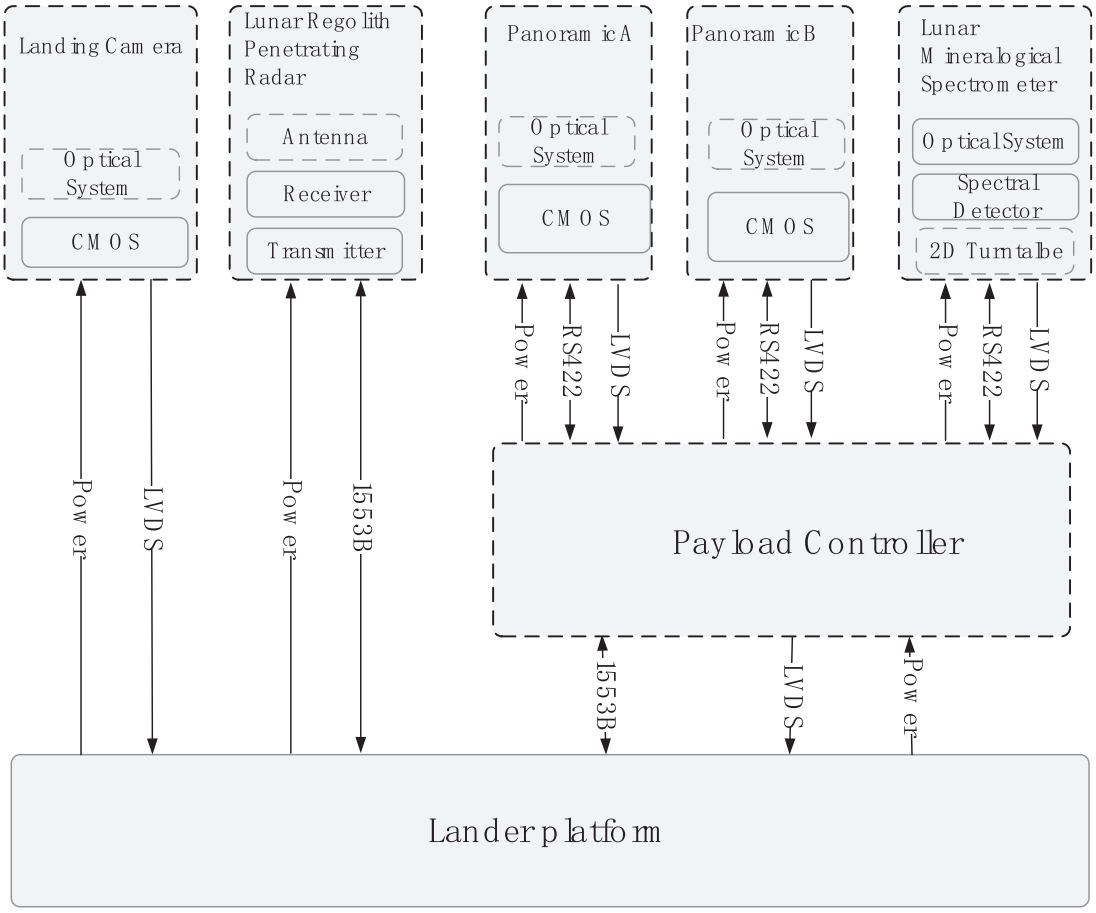

Fig. 6. The Framework of scientific payload system.

mode 1 works for 5 s, mode 2 works for 1 s and completes a cycle in 6 s. The image of mode 2 is transmitted back to the Earth in real time, and the image of mode 1 is transmitted back to the Earth after landing on the moon.

The Lunar Regolith Penetrating Radar: there are two working modes, internal calibration mode and detection mode. Before drilling, the Lunar Regolith Penetrating Radar is powered up to carry out internal calibration and scientific detection, and takes 32 min to carry out a complete probe (for 128 cumulative times). Multiple detection can be performed according to the needs of the detection tasks.

The Panoramic camera: There are two modes, static imaging and dynamic camera. Before and after shoveling sample collection, the panoramic camera takes images in the whole field of view respectively, and takes 120 pictures for each imaging, acquiring 240 pictures.

The Lunar Mineralogical Spectrometer: There are calibration mode, full-band acquisition mode, short-wave full-field-of-view acquisition mode, mid-wave full-field-of-view acquisition mode, visible and near-infrared full-field-of-view acquisition mode, etc. The spectral detection of sampling points is performed before and after the shoveling sample collection, respectively.

3.3. Scientific payload design

3.3.1. Landing camera

The landing camera is a high-performance, miniaturized optical imaging detection device that works in the lander powered descent section to acquire optical images of the landing area. It can also be used to analyze the topography and regional geology of the lunar surface in the landing area. Table 3 shows the main performance parameters of the landing camera.

The design of the landing camera adopts the integrated design of optical, structural, electronic system and temperature control. Optical system has a window glass, six high transmission lenses. Considering the requirements of the optical system of radiation protection, the first lens uses radiation-proof glass, optical system transmittance is about 0.87. Detector parts uses DALSA's IA-G3 CMOS image sensor parts, electronics composition is shown in Fig. 8. Focal plane circuit consists of CMOS image sensor and its peripheral circuit, mainly completes the function of photoelectric signal conversion. Video processing circuit mainly consists of FPGA, SDRAM and interface conversion chip, to complete the CMOS drive signal output, static image compression, automatic exposure and other func-

Fig. 7. The scientific payloads (from left to right, first row:Panoramic Camera, Lunar Mineralogical Spectrometer, second row:Landing Camera, Lunar Regolith Penetrating Radar Controller, third row: Antenna of Lunar Regolith Penetrating Radar A/B/C).

Table 3
Main performance parameters of the Landing Camera.

Items	Main performance parameters
Imaging distance (m)	4∼∞
Effective pixel number	Imaging mode 1:2352 × 1728, 4:1 compression; Imaging mode 2:1024 × 1024, 8:1 compression
Flied of view (°)	Imaging mode 1: 59°×45°; Imaging mode 2: 27.5°×27.5°
System static modulation transfer function	0.21
Maximum data rate (Mbps)	≦10
Mass (kg)	≦0.6
power (W)	≦10

tions. Power distribution circuit mainly conducts the primary and secondary power conversion, the implementation of switching instructions and other functions.

The landing camera had two working modes, Mode 1 and Mode 2. LCAM took images one frame per second, in Mode 1 it took image 5 frames then in Mode 2 it takes images 1 frame, working alternately. LCAM powered on and started working, images in Mode 2 were transmitted down to the ground in real time, and images in mode 1 were cached and transmitted back to the ground after the probe landed on the moon due to the limitation of the data transmission channel.

3.3.2. Lunar Regolith Penetrating Radar

LRPR is a subsurface penetrating detection radar installed on the Chang'e-5 lander platform, whose detection task is the detection of lunar subsurface structure and lunar soil thickness, and provides information support during the drilling sample process after the lander landing the lunar surface.

LRPR electronics box is installed inside the drilling side of the lander, and the antenna is installed at the bottom of the lander. LRPR adopts the carrier-free frequency picosecond pulse signal and uses 12 ultra-broadband time-domain antennas to form a transceiver multiplexed antenna array to achieve high-resolution detection images of the thickness of the lunar soil and its layered structure in the area below the antenna array by means of electrical scanning detection.

There are 12 transceiver antennas, divided into three groups A, B and C. Group A antennas consist of antennas numbered 1 to 7, group B antennas consist of antennas numbered 8 to 11 and group C antennas consist of anten-

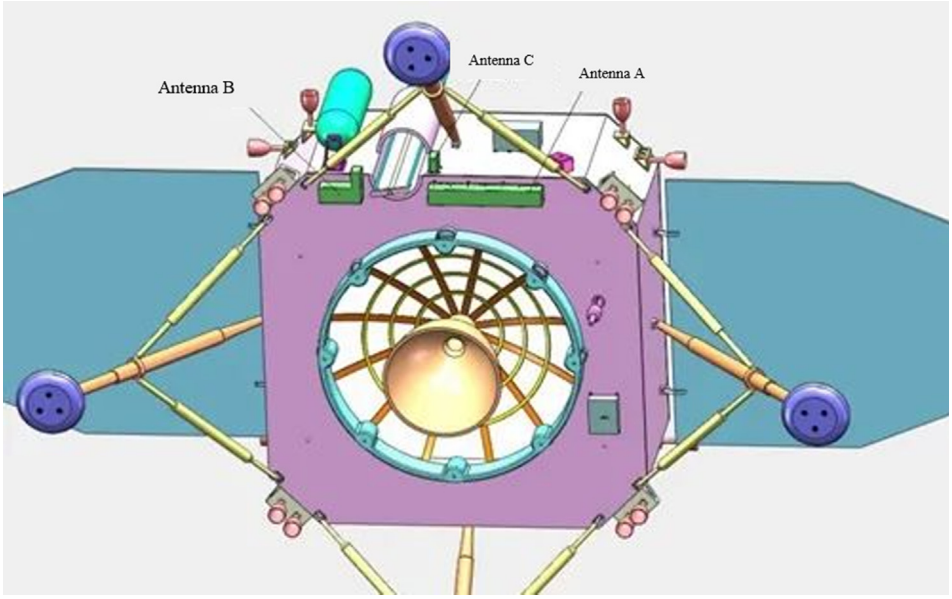

Fig. 8. The specific installation position of LRPR on the lander.

nas numbered 12. 3 groups of antennas are installed at the bottom of the lander, and the installation position is shown in Fig. 8. Each antenna can both transmit and receive electromagnetic pulse (EMP) signals. The EMP signal emitted by each antenna covers an elliptical area, and Fig. 9 shows the area covered by the EMP signal emitted by 12 antennas, and the drill bit of the drilling device is located at the intersection of the 12 covered areas. When one of the antennas transmits the pulse signal, the other 11 antennas receive the pulse signal reflected from the interior of the Moon in turn. 12 antennas finish transmitting and receiving in turn, and by analyzing all the received signals, the internal stratification structure of the shallow layer of the lunar surface below the antennas can be inverted, especially the internal structure of the lunar surface in the drilling area. It can provide technical support for drilling. Table 4 shows the main technical parameters of LRPR.

3.3.3. Panoramic camera

PCAM are installed on the sampling side of the lander, consisting of two cameras at 270 mm distance apart, which can achieve stereo imaging of the target through the detection principle similar to the "human eyes". Relying on the left and right rotation and up and down pitch of the rotating mechanism, they can achieve a panoramic detection on a large field of view and a wide range up and down, covering the sample collection area. Then through image stitching and stereo inversion, a panoramic stereo image of the sample collection area can be got.

As shown in Fig. 10, the panoramic camera is mounted on the rotating mechanism, the angle of orientation rotation is −90° to +90°, the angle of pitch rotation is −85° to +90°, the panoramic camera can achieve full coverage of the field of view of the sampling area with the cooperation of the rotating mechanism, as shown in Fig. 11, this is

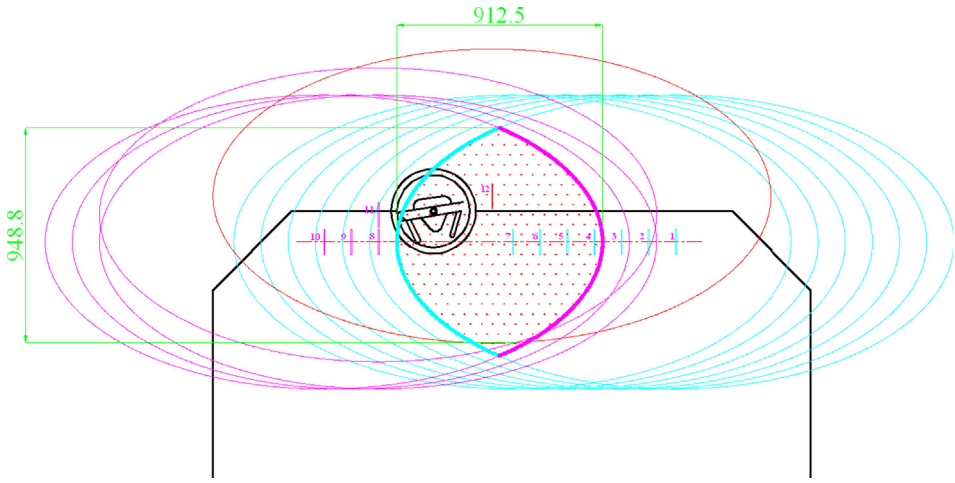

Fig. 9. The antenna footprint of LRPR.

the top view, the pink area indicates the sampling range of the robotic arm, the gray area indicates the panoramic camera field of view, the green area indicates the panoramic camera can achieve full coverage of the sampling area of the robotic arm within the rotation range of the rotating mechanism.

Table 4
Main performance parameters of the Lunar Regolith Penetrating Radar.

Items	Main performance parameters
Center frequency (MHz)	2000
Bandwidths (MHz)	≥2000
Depth (m)	≥2
Thickness resolution	Better than 5 cm
Detection range	Covering sample drilling area
Mass (kg)	≦4
Power (W)	≦15
Maximum data rate (bps)	≦1M

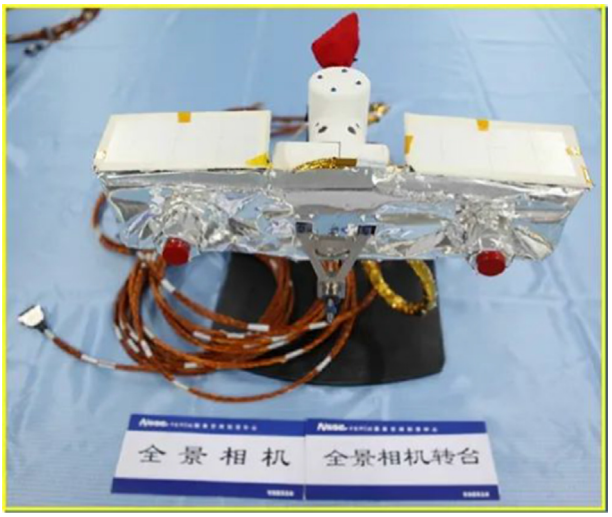

Fig. 10. Assembly picture of panoramic camera and rotating mechanism (range of rotating mechanism: azimuch angle: −90° to +90°, pitch angle: −85° to +90°).

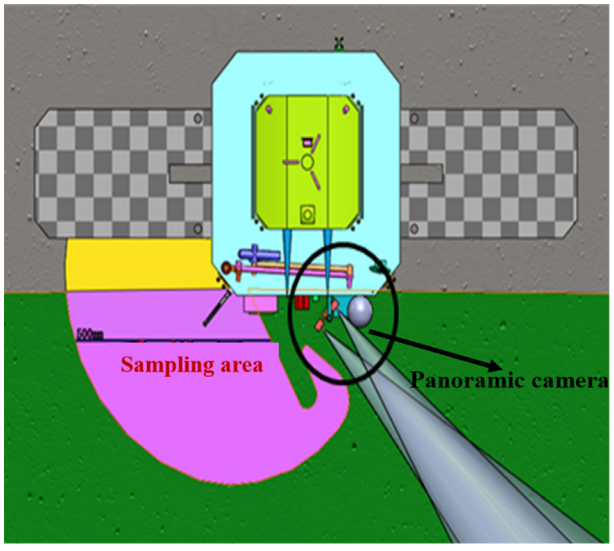

Fig. 11. The field of view simulation of the sampling area of the manipulator by PCAM.

PCAM consists of several parts, including optical system, mechanical system, electronics, and thermal control. The electronics part includes detector, camera power circuit, FPGA, SDRAM, RS422 bus interface and image output interface (LVDS).

When the sample collection mechanism works, PCAM can also take pictures and video of the sample collection process, so as to obtain the sample collection process image information, while cooperating with other scientific payloads to jointly complete the scientific objectives of the sample collection area in situ detection. Table 5 is the main performance parameters of PCAM, Fig. 10 is the installation picture of the panoramic camera on the turntable. The field of view simulation of the sampling area of the manipulator by PCAM is shown in Fig. 11.

3.3.4. Lunar Mineralogical Spectrometer

LMS is installed on the side panel of the lander located below the lander's robotic arm. By changing the driving

Table 5
Main performance parameters of the Panoramic Cameras.

Items	Main performance parameters
Color	Color RGB
Band range	Visible spectrum (420–700 nm)
Imaging distance (m)	0.5 m–∞
Effective pixels number	2352 × 1728
Diagonal viewing angle (°)	24.1
System static modulation transfer function	0.31
Signal to noise ratio (dB)	≧40 (Maximum signal to noise ratio) ≧30 (albedo 0.09, sun elevation 30°)
Field distortion	Better than 1% (full field of view)
Mass (kg)	≦0.6
Power (W)	≦3
Maximum data rate (bps)	40 M + 40 M

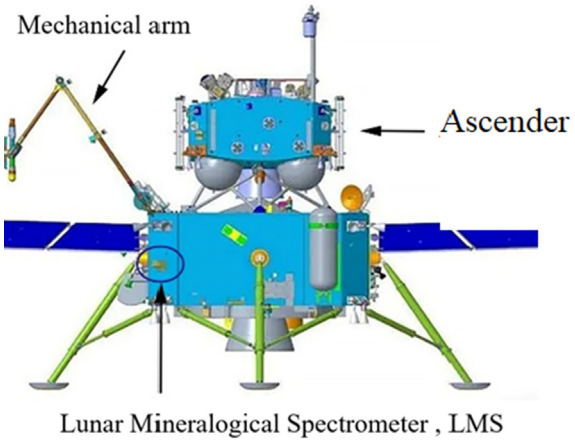

Fig. 12. The location of LMS installed at the lander. The mechanical arm completes the work of shoveling samples by selecting points of scientific value through the spectral detection of LMS.

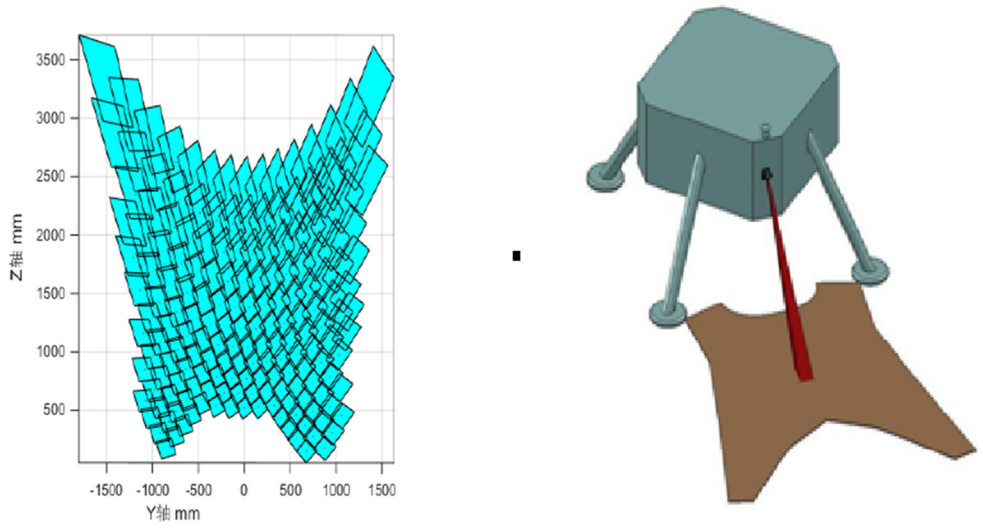

Fig. 13. Simulation diagram of lunar mineral spectrometer detection range.

frequency of the acousto-optic tunable filter (AOTF), the wavelength of the light waves passing through the AOTF got changed. The desired spectral curve and the spectral image of the specified wavelength are finally obtained. At the same time, by integrating the designed two-dimensional rotating pointing mechanism (pitch angel: 0° to +30°, azimuth angle: –22.5° to +22.5°), the pointing mirror is rotated as required to realize the pointing adjustment detection of the sampling point, thus meeting the tasks of multi-point detection of the sample collection area. Fig. 12 shows the installation position of LMS on the lander. Through the spectral detection of LMS, the points with scientific value are selected, and then the mechanical arm completes the work of shoveling the lunar samples. Fig. 13 shows the simulation diagram of the detection range of LMS.

Table 6
Main performance parameters of the Lunar Mineralogical Spectrometer.

Items	Main performance parameters
Spectral range (nm)	480–3200
Spectral resolution (nm)	2.4–24.8
Field of view (°)	4.1 × 4.1
Detection distance (m)	1.7–5
Signal to noise ratio (dB)	≧40 (Maximum signal to noise ratio) ≧30 (albedo 0.09, sun elevation 45°)
Mass (kg)	≦5.73
Power (W)	≦15.2
Maximum data rate (bps)	≦800

LMS consists of the following parts, including the dust protection device, the two-dimensional rotation pointing mechanism, the optical part, and the electronics part. The AOTF beam splitting component can select the splitting wavelength by changing the driving RF frequency. The converging mirror converges the parallel beams from the AOTF spectrometer on the detector assembly to achieve the purpose of spectral detection and spectral imaging. The RF driver assembly realizes Hz-level frequency adjus-

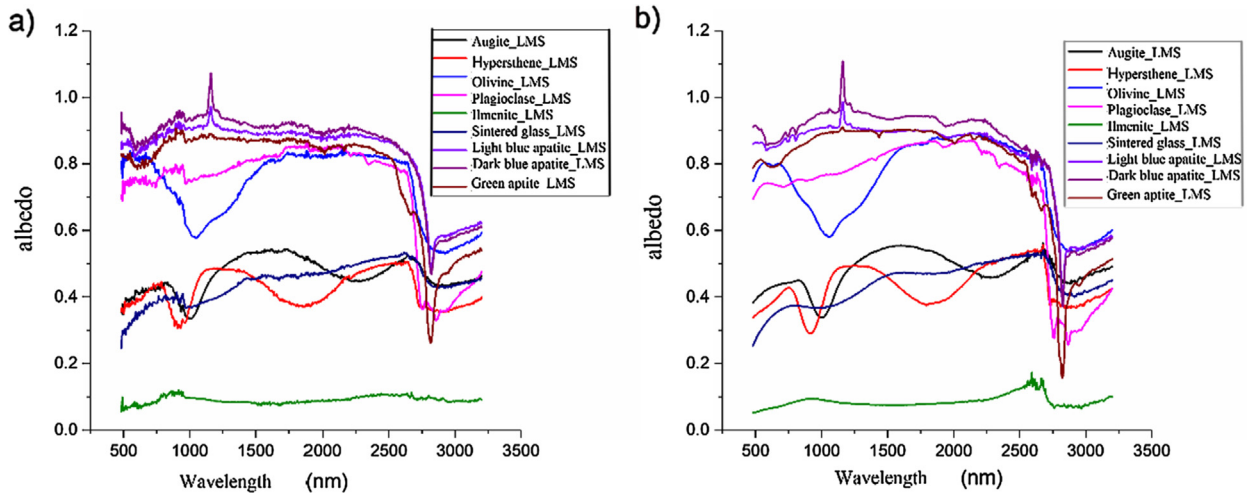

Fig. 14. The comparison of the full-band spectral curves of the samples measured by LMS with the standard comparison instruments ASD and DP102F.

table RF power drive to complete the function of spectral refinement of the reflected broad-spectrum light to achieve the selection of the spectral wavelength.

Table 6 shows the main performance parameters of the LMS, Fig. 14 shows the comparison of the full-band spectral curves of the samples measured by LMS with the standard comparison instruments ASD and DP102F, both in terms of spectral shape and reflectance amplitude are in good agreement, which can effectively identify the spectral characteristics and absorption peak characteristics of the samples (He et al., 2020). By comparing the common pyroxene with obvious absorption peak characteristics, the data quality meets the requirements of the task and application by calculating the error of the center position of absorption peaks of common pyroxene and peridotite samples with obvious absorption peak characteristics (Ting-ni et al., 2019).

4. On-orbit operation of scientific payloads

CE-5 mission landed in the Mons Ruemker region (43.1° N, 51.6° W) of northern Oceanus Procellarum on December 1, 2020 at 23:11 Beijing time. The Landing Camera (LCAM) started to power up when it was 17 km away from the lunar surface, and transmitted 1024 × 1024 resolution image in real time, which helped the lander-ascender

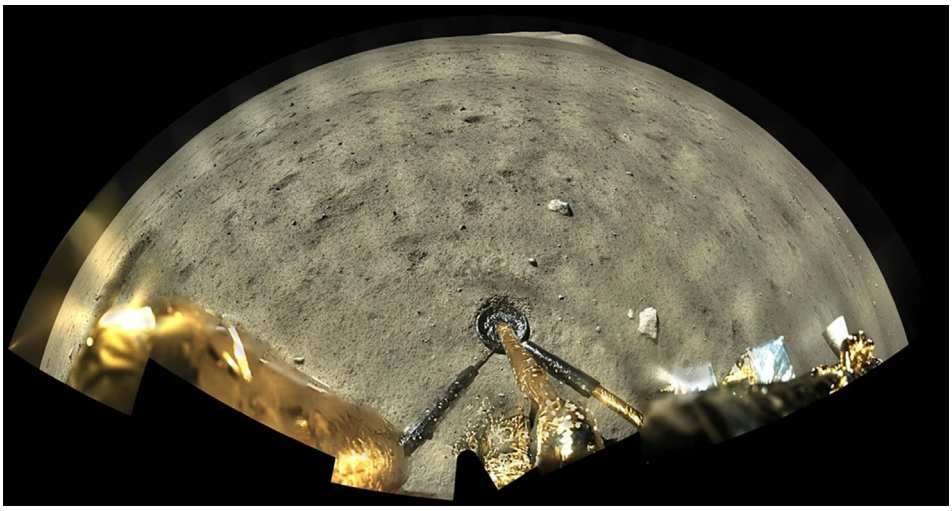

Fig. 15. A color panoramic image of the sampling area of the CE-5 taken by panoramic camera.

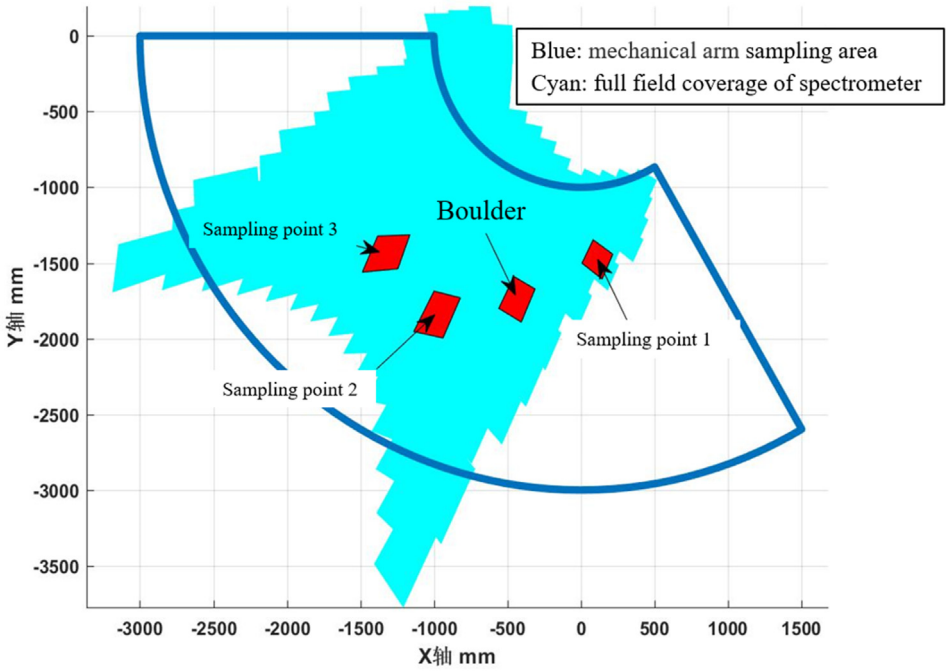

Fig. 16. Full field coverage of spectrometer (blue trapezoidal area). The three selection points are shown in the figure.

combination to land safely. During the landing progress, the LCAM captured 649 images with 2352 × 1728 resolution, 129 images with 1024 × 1024 resolution. After landing on the lunar surface, the data was sent back to the earth. After processing, the dynamic image of the probe landing on the moon was formed.

On December 1, 2020, before drilling and sampling, LRPR started to work on detecting the lunar soil structure of drilling point and identifying the layered structure. After drilling, three more detections were carried out to further explore and analyze the underground structure of the landing site. The original plan for CE-5 mission was to drill to a depth of 2 m. According to the analysis of the detection results of the lunar soil structure detector, there were large rocks at a depth of 1 m from the lunar surface, so the drilling and sampling stopped at a depth of 0.9 m.

After drilling, shoveling collection were conducted. Firstly, PCAM took a panoramic image of the landing area, shown as Fig. 15.

Based on the analysis of the panoramic image, with the range of motion of the shovel manipulator and the view of the LRPR, the schematic diagram of the sampling points was designed as shown in Fig. 16. Finally, a total of 12 shovels were made at 3 points. The LMS conducted spectral measurement during the whole process-before, during and after shoveling.

5. Conclusions

This paper mainly focuses on the scientific objectives and exploration tasks of CE-5, carries out the design of CE-5 scientific payload system architecture design and individual scientific payload design, payload technical indicators analysis, working mode design and detection viewing field analysis. Through the design and analysis results, scientific payloads carried out the preliminary geological background study of the sampling area, which effectively supported the sample collection work of CE-5 on the lunar surface and successfully completed the specified exploration mission.

CE-5, which was launched half a century later, carried four scientific payloads to obtain scientific data for in-situ exploration of the landing area and carried out analysis and research on the background characteristics of the landing area. Through the collection of lunar samples, it will carry out laboratory research on the physical and chemical properties of lunar samples, the mechanism of formation and evolution of lunar soil and the history of lunar chemical evolution, providing scientific answers for a profound understanding of the formation of the Earth-Moon system and the evolutionary history of the formation of the solar system.

Declaration of Competing Interest

The authors declare that they have no known competing financial interests or personal relationships that could have appeared to influence the work reported in this paper.

Acknowledgement

This research was funded by the National Key R&D Program of China (Grant NO. 2020YFE0202100), the Key Research Program of the Chinese Academy of Sciences, Grant NO. ZDRW-KT-2019-5, the National Science Foundation of China (Grant No. 41590851, 11941001, 42072337), the Beijing Municipal Science and Technology Commission (Grant No. Z181100002918003), and by the Pre-research project on Civil Aerospace Technologies No. D020201 and No. D020203 funded by China National Space Administration (CNSA).

References

Chen, ChunLiang, Zhang, ZhengFeng, Peng, Jing, Zhang, Wu, Zhang, Gao, Yang, MengFei, Du, Ying, Wang, Yong, Wang, XiaoLei, 2015. Technique design and realization of the circumlunar return and reentry spacecraft of 3rd phase of Chinese lunar exploration program (in Chinese). Sci. Sin. Tech. 45 (2), 111–123. https://doi.org/10.1360/N092014-00484.

Fa, Wenzhe et al., 2014. Regolith thickness over Sinus Iridum: Results from morphology and size-frequency distribution of small impact craters. J. Geophys. Res. Planets 119 (8), 1914–1935.

Fa, Wenzhe, Zhu, Meng-Hua, Liu, Tiantian, Plescia, Jeffrey B., 2015. Regolith stratigraphy at the Chang'E-3 landing site as seen by lunar penetrating radar. Geophys. Res. Lett. 42 (23). https://doi.org/10.1002/grl.v42.2310.1002/2015GL066537.

Geologic map of the Rumker quadrangle of the Moon, Scott D H, Eggleton R E. http://pubs.er.usgs.gov/publication/i805/ [2020-02-18].

He, Z., Li, J., Li, C., Xu, R., 2020 Jan. Measurement and Correction Model for Temperature Dependence of an Acousto-Optic Tunable Filter (AOTF) Infrared Spectrometer for Lunar Surface Detection. Appl. Spectrosc. 74 (1), 81–87. https://doi.org/10.1177/0003702819881786, Epub 2019 Nov 8 PMID: 31617383.

He, Fei, Zhang, Xiao-Xin, Chen, Bo, Fok, Mei-Ching, Zou, Yong-Liao, 2013. Moon-based EUV imaging of the Earth's Plasmasphere: Model simulations. J. Geophys. Res. Space Physics 118 (11), 7085–7103. https://doi.org/10.1002/2013JA018962.

Jia, Yingzhuo, Zou, Yongliao, Ping, Jinsong, Xue, Changbin, Yan, Jun, Ning, Yuanming, 2018. The scientific objectives and payloads of Chang'E−4 mission. Planet. Space Sci.

Jianjun, Liu, Xin, Ren, Lingli, Mou, Liyan, Zhang, Jianqing, Feng, Xiaoduan, Wang, Chunlai, Li, 2013. Payloads and Scientific Experiments of Chang'E-2 Lunar Orbiter. Life Sci. Instrum. 11 (Z1), 31–38.

Jian-Zhong, Liu, Zi-Yuan, Ouyang, Chun-Lai, Li, Yong-Liao, Zou, 2013. China National Moon Exploration Progress (2001-2010). Bull. Mineral. Petrol. Geochem. 32 (05), 544–551.

Ling, Zongcheng, Qiao, Le, Liu, Changqing, Cao, Haijun, Bi, Xiangyu, Lu, Xuejin, Zhang, Jiang, Fu, Xiaohui, Li, Bo, Liu, Jianzhong, 2019. Composition, mineralogy and chronology of mare basalts and non-mare materials in Von Kármán crater: Landing site of the Chang'E−4 mission. Planet. Space Sci. 179, 104741. https://doi.org/10.1016/j.pss.2019.104741.

Luan, E.J., 2006. China's lunar exploration program the third milestone for China's space industry. Eng. Sci. 8 (10), 31–36.

Mallapaty, Smriti, 2020. China set to retrieve first Moon rocks in 40 years. Nature 587 (7833), 185–186.

Mc Dowell, J., A Merge of a Digital Version of the List of Lunar Craters from NASA Catalogue of Lunar Nomenclature with the List from the USGS Site [DB/OL]. http://www.planet4589.org/astro/lunar/Crater.

Ouyang, Ziyuan, Jiang, et al., 2008. Preliminary Scientific Results of Chang'E-1 Lunar Orbiter: Based on Payloads Detection Data in the First Phase. Chin. J. Space Sci. 5, 361–369.

Qian, Y.Q., Xiao, L., Zhao, S.Y., Huang, J., Flahaut, J., Martinot, M., Head, J.W., Hiesinger, H., Wang, G.X., 2018. Geology and Scientific Significance of the Rumker Reginon in Northern Oceanus Procellarum: China''s Chang''E-5 Landing Region. J. Geophys. Res. Planets.

Qian, Yuqi, Xiao, Long, Yin, Shen, Zhang, Ming, Zhao, Siyuan, Pang, Yong, Wang, Jiang, Wang, Guoxin, Head, James W., 2020. The regolith properties of the Chang'e-5 landing region and the ground drilling experiments using lunar regolith simulants. Icarus 337, 113508. https://doi.org/10.1016/j.icarus.2019.113508.

Qiao, Le, Xiao, Long, Zhao, Jiannan, Huang, Qian, Haruyama, Junichi, 2014. Geological features and evolution history of Sinus Iridum, the Moon[J]. Planet. Space Sci. 101, 37–52.

Ting-ni, C., Chun-lai, L., Zhi-ping, H., Xin, R., Bin, L., Rui, X., 2019. Experimental Ground Validation of Spectral Quality of the Chang'E-5 Lunar Mineralogical Spectrometer. Spectrosc. Spectr. Anal. 39 (01), 257–262.

Wang, J., Deng, J.S., Cui, J., Cao, L., Qiu, Y.L., Wei, J.Y., 2011. Lunar exosphere influence on lunar-based near-ultraviolet astronomical observations. Adv. Space Res. 48 (12), 1927–1934.

Ye, PeiJian, Yang, MengFei, Huang, JiangChuan, Meng, LinZhi, Sun, ZeZhou, 2014. The process and experience in the development of Chinese lunar probe (in Chinese). Sci. Sin. Tech. 44 (6), 543–558. https://doi.org/10.1360/N092014-00150.

Zhang, Aibing, Wieser, Martin, Wang, Chi, Barabash, Stas, Wang, Wenjing, Wang, Xiaodong, Zou, Yongliao, Li, Lei, Cao, Jinbin, Kalla, Leif, Dai, Lei, Svensson, Johan, Kong, Linggao, Oja, Magnus, Liu, Bin, Alatalo, Vesa, Zhang, Yiteng, Talonen, Juha, Sun, Yueqiang, Emanuelsson, Magnus, Xue, Changbin, Wang, Lei, Wang, Fang, Liu, Wenlong, 2020b. Emission of energetic neutral atoms measured on the lunar surface by Chang'E-4. Planet. Space Sci. 189. https://doi.org/10.1016/j.pss.2020.104970, ISSN 0032-0633.

Zhang, S., Wimmer-Schweingruber, R.F., Yu, J., Wang, C., Fu, Q., Zou, Y., Sun, Y., Wang, C., Hou, D., Böttcher, S.I., Burmeister, S., Seimetz, L., Schuster, B., Knierim, V., Shen, G., Yuan, B., Lohf, H., Guo, J., Xu, Z., Freiherr von Forstner, J.L., Kulkarni, S.R., Xu, H., Xue, C., Li, J., Zhang, Z., Zhang, H., Berger, T., Matthiä, D., Hellweg, C.E., Hou, X., Cao, J., Chang, Z., Zhang, B., Chen, Y., Geng, H., Quan, Z., 2020b. First measurements of the radiation dose on the lunar surface. Sci. Adv. 6, eaaz1334.

Zhao, JianNan, Huang, Jun, Qiao, Le, Xiao, ZhiYong, Huang, Qian, Wang, Jiang, He, Qi, Xiao, Long, 2014. Geologic characteristics of the Chang'E-3 exploration region. Sci. China Phys Mech. Astron. 57 (3), 569–576.

Zhaoyu, Pei, Qiong, Wang, Yaosi, Tian, 2015. Technology Roadmap for Chang'E Program. J. Deep Space Explor. 2 (02), 99–110.

Zhihao, Pang, 2021. Chang'e 5 Returns Home with Lunar Samples. KEXUE 73 (01), 34–38.